Bulletin of Engineering Geology and the Environment (2022) 81: 1
https://doi.org/10.1007/s10064-021-02521-x

ORIGINAL PAPER

Experimental investigation on the transmissivity of fractured granite filled with different materials

Qun Sui[1,2] · Diansen Yang[1,2] · Weizhong Chen[1,2] · Shengqi Yang[3]

Received: 6 April 2021 / Accepted: 14 November 2021 / Published online: 8 December 2021

Abstract

The disposal of high-level radioactive waste (HLW) is one of the most challenging issues globally, and granite is considered an ideal host rock. In this paper, we present an experimental study on the transmissivity of fractured granite filled with different materials. A series of tests were carried out to study the effects of different factors (filling material, confining stress, and fracture roughness) on fracture transmissivity. Our results show that the properties of the filling material play a critical role in the transmissivity of fractured granite. Specifically, quartz sand significantly increases the transmissivity of the fractured granite, but the larger the sand particle size, the slower the transmissivity increases. Conversely, compared with fractured samples without any filling material, bentonite as a filling material decreases fracture transmissivity. Furthermore, confining stress also exhibits a great effect on transmissivity, and high stress compresses the filling material, resulting in a reduction in transmissivity. In addition, confining stress has a larger impact on the transmissivity of sand-filled fractured samples than others. We quantify the roughness of the fractures to examine its impact on the transmissivity. The results show that larger roughness reduces transmissivity for the unfilled fractures, but has an opposite effect on sand-filled fractures, while the results of bentonite-filled fractures are scattered. This study could provide an important guidance for evaluating the safety of HLW repositories.

Keywords Fractured granite · Transmissivity · Filling material · Confining stress · Fracture roughness

Introduction

Granite is considered to be an ideal host rock for high-level radioactive waste (HLW) geological disposal (Wang et al. 2006, 2018) because of its low permeability, high strength, and good thermal conductivity. Understanding the transport properties of fractured granites is one of the key issues for the assessment of feasibility and safety of long-term HLW disposal (Yang et al. 2017, 2018).

✉ Diansen Yang
dsyang@whrsm.ac.cn

[1] State Key Laboratory of Geomechanics and Geotechnical Engineering, Institute of Rock and Soil Mechanics, Chinese Academy of Sciences, Wuhan, Hubei 430071, People's Republic of China

[2] University of Chinese Academy of Sciences, Beijing 100049, People's Republic of China

[3] State Key Laboratory for Geomechanics and Deep Underground Engineering, School of Mechanics and Civil Engineering, China University of Mining and Technology, Xuzhou 221116, People's Republic of China

A large number of studies have been carried out to understand the effects of stress on permeability in fractured granites. It is well documented that permeability strongly depends on confining stress and stress path (Vogler et al. 2016; Yang et al. 2019; Yin et al. 2019). Several empirical formulae (e.g., exponential function) have been proposed to quantify the relationship between permeability and the applied stress (Olsson and Barton 2001; Min et al. 2004; Alam et al. 2014; Majid and Lanru 2015; Wang et al. 2015). Fracture roughness is another factor influencing the permeability, which causes the variation of fracture aperture and potential transition of flow regimes (Coli et al. 2008; Liu et al. 2016; Wang et al. 2016; Wu et al. 2020). Yong et al. (2018) proposed a method to determine the maximum sampling interval in the measurement of two-dimensional joint roughness by studying the sensitivities of several widely used roughness parameters to the sampling interval. Numerical investigations show that geometric fracture characteristics (e.g., aperture, length, and surface roughness) play an important role in the permeability of the fractured rock mass (Alireza and Lanru 2007, 2008; Liu et al. 2016, 2018; Mu

et al. 2019; Zhang et al. 2021). Early studies have shown that fillings in the fractures can alter the mechanical behavior and transport properties of fractures. Filling materials in natural rock joints may reduce the shear strength of the joints and affect the stability of rock masses (Indraratna et al. 2005, 2008; Shrivastava and Rao 2017; Cheng et al. 2018). Some studies have demonstrated that the permeability of fractures is significantly affected by the presence of the fillings (Chen and Kinzelbach 2002; Olson et al. 2009; Wang et al. 2010, 2019; Rutqvist 2015; Yu et al. 2015; Khosravi et al. 2016; Lu et al. 2016; Liu et al. 2017, 2019; Cheng et al. 2018). Wealthall et al. (2001) found that, compared to fractures filled with a small amount of filling material, permeability behaves oppositely in fractures filled with a large amount of material. Ye et al. (2019) established an equivalent permeability coefficient model for partially filled fractures to investigate the dependence of permeability on the degree of filling in the fractures. In recent years, significant work has been devoted to understanding the effect of proppants on the hydraulic conductivity of fractures in geothermal energy recovery, exploitation of oil and gas resources, and transport of pollutants in rock masses (Zheng et al. 2016; Bandara et al. 2020; Suri et al. 2020). The results of experiments and numerical simulations show that fracture conductivity increases with increasing proppant concentration and proppant particle size, and reducing closure stress (Hou et al. 2017; Li et al. 2018; Zheng et al. 2018; Xu et al. 2019; Zhu et al. 2019; Liang et al. 2021; Xiao et al. 2021). However, the influence of fillings materials in the fracture on the transmissivity of fractured granite remains largely unclear.

This paper aims to study the evolution of transmissivity in single fractures with different filling materials under confining stress. Specifically, we will explore the impacts of fracture roughness, confining stress, and filling conditions on the transmissivity of fractured granite.

Experiment preparation

Specimen preparation

Granite was collected from Rizhao in Shandong province, China, to investigate the transmissivity of filled fractured granite. In this experiment, all specimens were cored from the same block of granite, with a diameter of ~ 50 mm and a length of ~ 70 mm. Based on the X-ray diffraction (XRD) results, the mineral components of this granite were quartz (11.12%), feldspar (59.85%), biotite (21.56%), amphibole (6%), chlorite (1.01%), and dolomite (0.46%). The grain size ranged from 6 to 18 mm, based on which it was classified as a coarse-grained granite (Yang et al. 2017, 2018).

To create a rough fracture surface, as shown in Fig. 1(a), the specimens were placed centrally in a mold equipped with a chisel edge or burin with which it was in contact. Clamping screws prevented the specimen from sliding and were aligned with the metal plate above the sample. A loading machine applied uniaxial preloading to the specimen, after which the clamping were removed so that during further loading, the specimen was in an unconfined state until the specimen was split in two halves along an axial fracture, as shown in Fig. 1(b).

Because the internal mineral distribution of each specimen varied, the planarity of each fracture surface was different, resulting in specimens with different fracture roughnesses. Figure 2 shows an example of a fractured specimen. The dimensions of all specimens are provided in Table 1.

Fig. 1 The preparation of specimens

Fig. 2 An example of a fractured granite specimen

Properties of the filling materials

According to previous studies (Tian 2013), the type of filling material in the fractured granite in the planned Beishan HLW storage area, Gansu, China, is similar to that in Matagami/Norita, Canada, (Blyth et al. 2009) and consisted mainly of calcite, quartz, and clay (mostly montmorillonite). Researchers worldwide have suggested that bentonite should be used to fill fractures in granite for waste repositories (Liu and Chen 2001; Push 2002). In view of this experience, quartz sand and bentonite were used as filling materials on the fracture transmissivity in these tests.

Quartz sand is a commonly used proppant for hydraulic fracturing around the world. Relevant studies have shown that the crushing strengths of 40/70 mesh and 70/140 mesh quartz sand in China are respectively 4000 psi and 5000 psi (about 27.6 MPa and 34.5 MPa) (Zheng et al. 2021). As shown in Fig. 3, quartz sand with a customized mesh ranges of 50 mesh (particle size ~ 0.25–0.3 mm), 100 mesh (particle size ~ 0.106–0.15 mm), and 200 mesh (particle size ~ 0.053–0.075 mm) were used.

Following the earlier study of Liu et al. (2007), the main mineral of the Gaomiaozi bentonite used in this research was 64 to 81% montmorillonite. The expansion capacity of this material was about 29.25 ml/g, that is, access to water resulted in 30 times volumetric free expansion. Due to the influence of viscous water film possessed by hydrated bentonite, its small particle size, and swelling capability, the permeability of bentonite is very low, and this decreases significantly with increase of compaction density.

Table 1 The dimensions of all specimens

Specimen number	Diameter (mm)	Length (mm)	JRC
No.1	47.92	70.52	13.01
No.2	47.88	70.67	13.50
No.3	47.65	70.32	13.97
No.4	48.24	71.20	14.39
No.5	47.44	70.52	14.84

Surface scan

Fracture surfaces of the specimens were scanned with a laser device to provide 3D coordinates (XYZ) for a large number of points. These scanned data were used to generate digitized fracture surfaces for the specimens (Fig. 4), and the joint roughness coefficients (JRC) were be calculated for each specimen, using the following equations of Yang et al. (2001) and Yong et al. (2018):

$$z_2 = \left[\frac{1}{(n-1)(\Delta x)^2}\sum_{i=1}^{n-1} z_{i+1} - z_i\right]^{1/2} \quad (1)$$

$$JRC = 32.69 + 32.98 * \lg Z_2 \quad (2)$$

where Z_2 is the root mean square slope of the profiles based on the scanned data, z_i represents the coordinates of the fracture surface profile, n is the number of data points, and Δx is the interval between the data points. The mean JRC values for the samples are listed in Table 1. It was noted that as the roughness increased, the undulation of the surface increased.

Fig. 3 The infilling materials used in this work

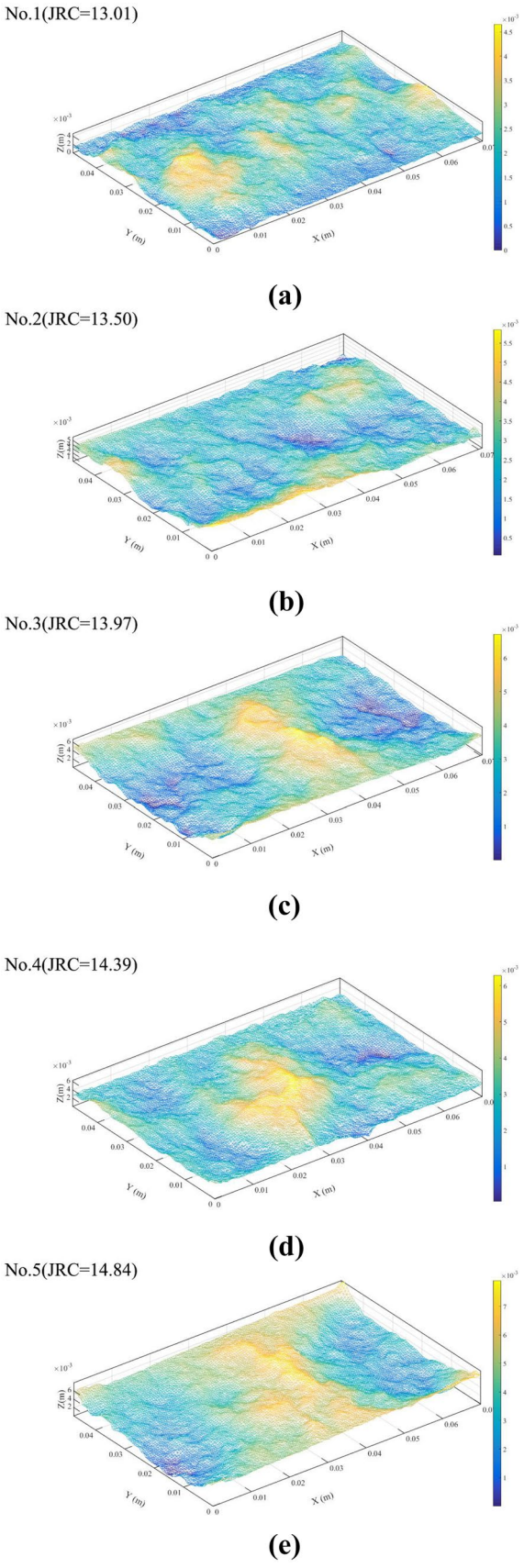

Fig. 4 3D scans for the fracture surfaces

Methods and procedures

As Fig. 5 shows, the apparatus was equipped with three independent pressure systems: axial stress, confining stress, and pore pressure, all supplied by ISCO pumps. In addition, the rock sample was tightly wrapped in a rubber sleeve under confining stress to ensure that the pore fluid only passed through the fracture in the sample.

To measure the transmissivity of the fractured granite samples, the steady-state method was preferred because of its better accuracy. The injection fluid was pumped in from the left side of the core chamber and passed through the sample to the right side. The injection pressure was recorded by a pressure sensor, and a balance set at the flow outlet recorded the mass of water flowed through the sample, from which the flow rate Q was calculated. An early study had shown that the porosity of the intact granite was only 0.825% (Yang et al. 2017). As the permeability of fracture was much higher than that of intact granite, the influence of permeability of the intact granite (i.e., matrix) was not considered in this study. Following Darcy's law, the flow rate ($\boldsymbol{Q}$) through porous media at a low velocity can be written as (Zimmerman and Bodvarsson 1996):

$$\boldsymbol{Q} = \frac{\boldsymbol{kA\Delta P}}{\boldsymbol{\mu L}} \tag{3}$$

where Q is the flow rate (m^3/s), μ is the dynamic viscosity of water ($\boldsymbol{PA \bullet s}$), k is the permeability (m^2), A is the cross-section area (m^2), and ΔP is the pressure difference (Pa), L is the length of the sample (m).

Generally, the ability of a fracture to transmit fluids is quantified by its transmissivity (T), which is equal to the product of the permeability and the area:

$$\boldsymbol{T = kA = \frac{\mu QL}{\Delta P}} \tag{4}$$

All tests were conducted at a constant temperature of 23 C, in order to evaluate the stress-dependent permeability of the fractured granite, with different confining stresses, axial stresses, and pore pressures during the experiment.

Five filling conditions (i.e., no filling, 50-mesh particle size sand, 100-mesh particle size sand, 200-mesh particle size sand, and bentonite) were selected. First, to ensure that the same filling quality was used under each operating condition, 0.3 g of each filling material was accurately weighed and evenly spread on the fracture surface by hand or using small brush (Fig. 6). The sample was weighed before and after filling to ensure that no filling material was lost during this process and to check the same amount of filling material was used under each condition. The half sample with filling material was matched with the appropriate other half and then wrapped together with adhesive tape to prevent

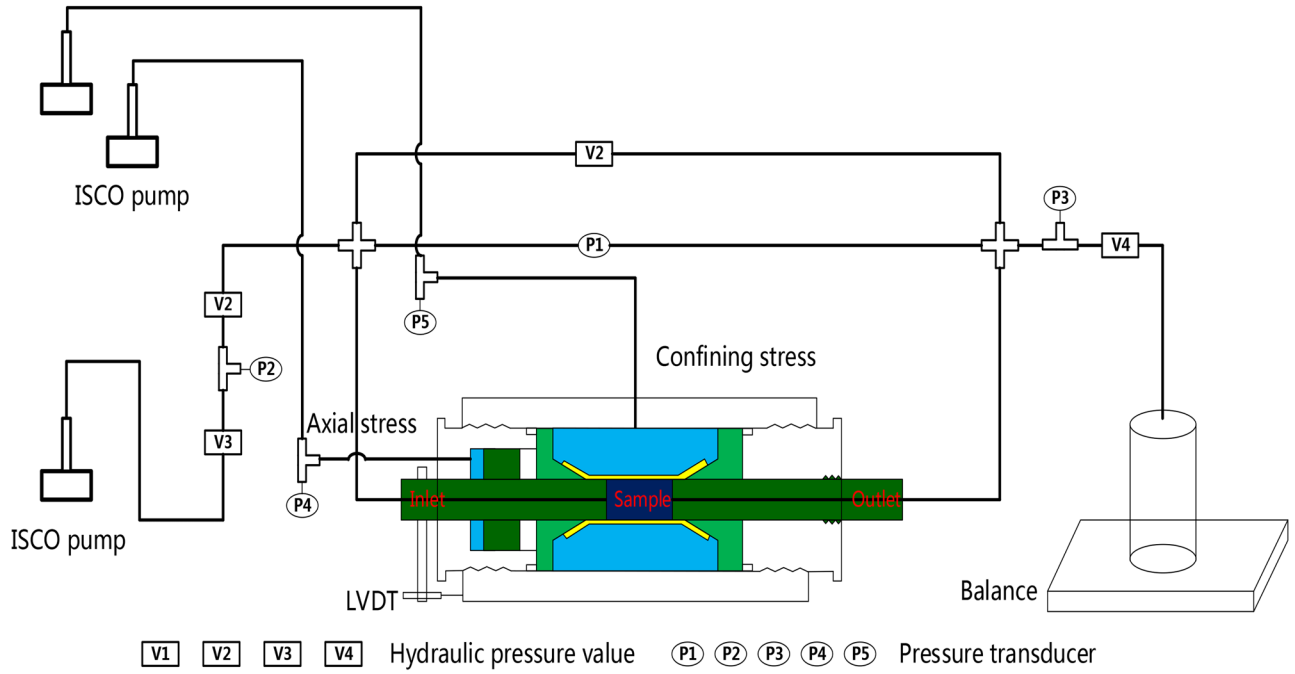

Fig. 5 The schematic diagram of the experimental apparatus

the escape of filling material from the fracture, as shown in Fig. 7(a). The samples were kept horizontal throughout the whole process to prevent the filling material from leaking out from the ends. As illustrated in Fig. 7(b), when the sample was placed in the core chamber, permeable stone plates were placed at both ends of the sample. These were held against the ends of the sample by the application of an axial stress to prevent filling material from escaping and only water was allowed to pass through the samples.

Pan and Qian (2009) claimed that nuclear waste is mostly buried at depths of 300–1000 m underground. From the results of the in situ stress measurements at different depths at the Beishan nuclear waste repository in Gansu, China, the confining stresses used in the tests were 10 MPa, 12 MPa, and 15 MPa (Zhao et al. 2014; Wang et al. 2018). As mentioned earlier, the crushing strength of quartz sand is much larger than the applied confining stress, so it was not expected that quartz sand particles would be crushed under these confining stress levels. The confining stress would also have restricted the change of distribution of filler on the fracture surface, although this was not checked.

Fig. 6 A fracture surface with 50-mesh quartz sand

After the confining stress was applied and kept constant, five levels of pore pressure difference from 0.1 to 0.5 MPa were applied and the flow rates were measured. Before recording the data, the flow was kept for a period of time to ensure that the flowing lines were full of water and the fracture was saturated. The flow outlet was submerged directly in water in the collection device and did not come into contact with air. It is possible that without the use of a back-pressure at the outlet, there may have been dissolved air in the water that would have created air bubbles in the outlet tube, but none were observed. Figure 8 shows the loading procedures used in this work.

Results and discussions

Table 2 shows the transmissivities of the fractures in the 5 specimens under different confining stress and filling conditions. For example, under a confining stress of 10 MPa and a water pressure difference of 0.3 MPa, the transmissivities of Sample No.1 filled with 50-mesh sand, without filling material, and with bentonite were 3.28×10^{-17} m^4, 2.17×10^{-19}

Fig. 7 Measures to prevent the filling material from being flowed out: (**a**) tape wrapped round specimen, (**b**) stone discs at ends of specimen

m^4, and 5.89×10^{-21} m^4, respectively. It is clear that, under the same stress and pore pressure difference conditions, the transmissivity of the fracture filled with sand was much larger than that of fractures without filling and filled with bentonite. Other specimens had similar patterns, where in general, samples filled with 50-mesh sands have the highest transmissivity (in the order of 10^{-17} m^4) and bentonite filled fractures have the lowest transmissivity (in the order of 10^{-21} m^4).

Effect of filling material

As shown in Fig. 9(a)–(e), the transmissivity of the samples filled with bentonite is about one to two orders of magnitude lower than that of unfilled samples. The reason is because bentonite has a strong adsorption capacity to liquids. As a result, of the swelling of bentonite the fracture was clogged by the expanded bentonite, which resulted in the reduction in fracture transmissivity. Because of the influence of viscous water film in bentonite, the bentonite also plays a role in blocking water and reducing flow capacity, thus further reducing the transmissivity of the sample. The transmissivity of the fracture filled with sand was about one to three orders of magnitude higher than that of unfilled fractures. This is because of the sand particles prevented closure of the fracture. In addition, the pore structure formed by the filling material was the main flow channel, and the porosity of which was higher than an unfilled fracture since the large pore volume possessed by the sand increased the flow capacity of the fracture. Thus, the flow rate was increased accordingly, and the fracture transmissivity was significantly increased.

Figure 9 illustrates that the fracture transmissivity of samples filled with quartz sand was related to particle size where the smaller the particle size, the lower the transmissivity. For instance, when the particle size of the sand changed from 50 to 200 mesh under the same confining stress, the transmissivity of the fracture with the same roughness decreased by one order of magnitude, which can be well explained by the difference in pore sizes and pore volumes. Hence,

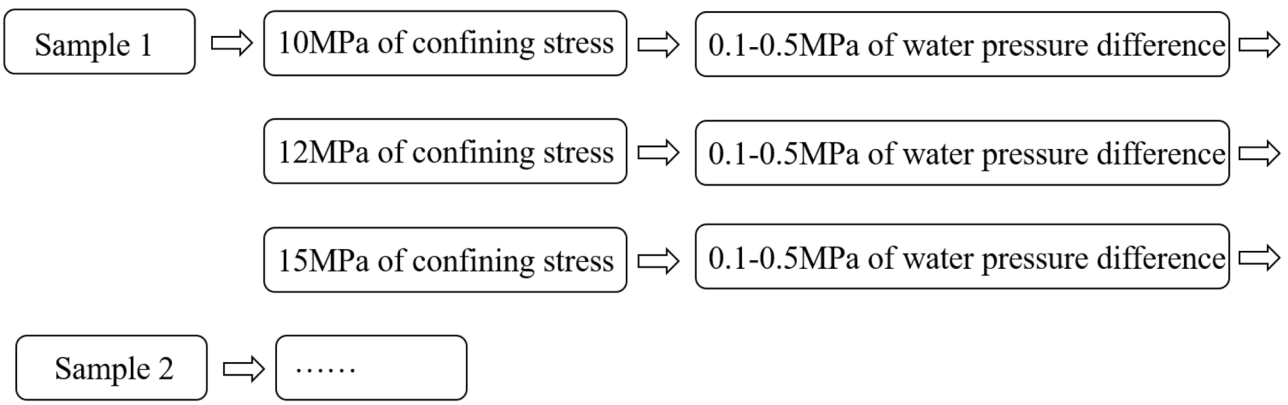

Fig. 8 The loading procedures of the experiment

Table 2 Transmissivity (m^4) of the samples

Sample	Confining stress (MPa)	Filling conditions				
		No filling	With particle 50mesh	With particle 100mesh	With particle 200mesh	With bentonite
No.1	10	2.17×10^{-19}	3.28×10^{-17}	1.11×10^{-17}	5.85×10^{-18}	5.89×10^{-21}
	12	9.50×10^{-20}	1.61×10^{-17}	5.98×10^{-18}	2.71×10^{-18}	2.17×10^{-21}
	15	4.85×10^{-20}	8.25×10^{-18}	3.76×10^{-18}	1.34×10^{-18}	8.10×10^{-22}
No.2	10	1.75×10^{-19}	3.48×10^{-17}	1.24×10^{-17}	3.53×10^{-18}	7.59×10^{-21}
	12	6.64×10^{-20}	1.72×10^{-17}	5.92×10^{-18}	2.25×10^{-18}	2.77×10^{-21}
	15	3.91×10^{-20}	5.45×10^{-18}	3.83×10^{-18}	1.09×10^{-18}	1.76×10^{-21}
No.3	10	1.67×10^{-19}	3.82×10^{-17}	1.59×10^{-17}	4.25×10^{-18}	5.05×10^{-21}
	12	6.04×10^{-20}	2.17×10^{-17}	8.09×10^{-18}	2.60×10^{-18}	2.20×10^{-21}
	15	3.58×10^{-20}	1.33×10^{-17}	4.85×10^{-18}	1.13×10^{-18}	9.03×10^{-22}
No.4	10	1.57×10^{-19}	4.23×10^{-17}	1.81×10^{-17}	4.09×10^{-18}	6.51×10^{-21}
	12	5.42×10^{-20}	2.70×10^{-17}	1.03×10^{-17}	2.05×10^{-18}	3.90×10^{-21}
	15	3.47×10^{-20}	1.69×10^{-17}	7.93×10^{-18}	1.44×10^{-18}	2.81×10^{-21}
No.5	10	1.59×10^{-19}	4.92×10^{-17}	2.16×10^{-17}	4.81×10^{-18}	4.38×10^{-21}
	12	5.12×10^{-20}	2.50×10^{-17}	8.16×10^{-18}	2.69×10^{-18}	2.24×10^{-21}
	15	3.20×10^{-20}	1.63×10^{-17}	3.84×10^{-18}	1.17×10^{-18}	1.06×10^{-21}

smaller sand particles form a denser pore structure, resulting in the reduction in flow capacity and fracture transmissivity. Furthermore, the smaller the sand particle size, the less the transmissivity varies with confining stress level. This occurs because the pore structure formed by quartz sand decreases with decreasing particle size. Therefore, during confining stress loading, the degree of compression of pore structure formed by smaller sand particles was lower and as a result, the difference of fracture transmissivity between different confining stresses was not so significant.

The experiments in this work show that filling conditions have the largest impact on fracture transmissivity. Although this phenomenon was reported before by other scholars, most of the earlier studies only considered one filling material. For instance, Liu et al. (2012a) found that the flow rate of an unfilled fracture was about 0.5 cm^3/s, which was lower than that of the fracture filled with coarse sand, at about 2.5 cm^3/s. Liu et al. (2010) and Liu et al. (2012a) also showed that the fracture permeability decreases as the size of filling material particle decreased, which is consistent with our study. Nara et al. (2017) explored permeability changes in fractures filled with clay and found that the permeability of unfilled fractures was about $10^{-16}\ m^2$ compared with filled fractures having a permeability of $10^{-18}\ m^2$, under the same water pressure and confining stress conditions. This difference of about two orders of magnitude is consistent with the results of this study.

Effect of confining stress

As shown in Fig. 10(a)–(c), the transmissivity of fractures decreased with increasing confining stress. In the first stage of confining stress loading (10–12 MPa), fracture transmissivity decreased rapidly, but the decline rate was reduced in the later stage (12–15 MPa). In this work, the ratio of fracture transmissivity reduction under confining stress from 10 to 12 MPa and 12 to 15 MPa with that under confining stress from 10 to 15 MPa was used to describe the reduction degree of fracture transmissivity in the initial and later loading stages respectively. Based on the calculation, for the five fractures with different roughnesses, in the initial stage of confining stress loading, the transmissivity reduction degree of fractures filled with 50-mesh quartz sand was 60 ~ 73%. However, in the later loading stage, the transmissivity reduction degree was 27 ~ 40%, showing a large difference compared with the initial loading stage. This trend holds true for other filling conditions. When the confining stress was increased by 5 MPa, the transmissivity of all samples was reduced by approximately one order of magnitude.

The influence of confining stress on the transmissivity of filled fracture was evident. In the first stage of confining stress loading, the fracture would have been the main flow channel, but as confining stress increased, the fracture aperture would be decreased and compression of the pore structure formed by the filling material would result in reduced porosity and the observed rapid reduction of fracture transmissivity. However, at the second stage of confining stress loading process, the filling material was already been compacted, irrecoverable plastic deformation and some particle crushing would have resulted in the destruction of the spatial structure of the medium and possibly cause blocking of the flow channels. However, it is likely that only minor particle crushing occurred at the second stage as the transmissivity reduction

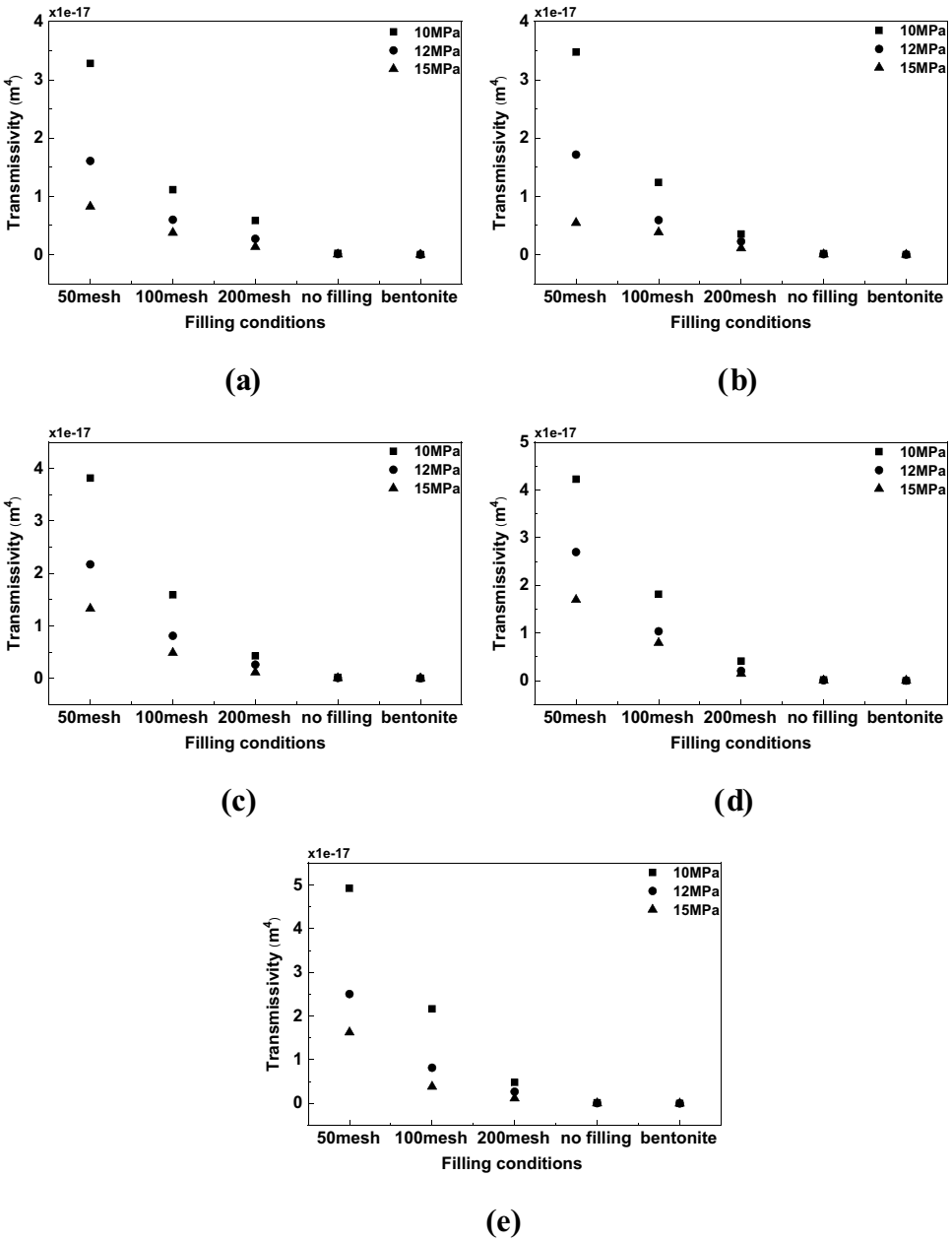

Fig. 9 Fracture transmissivity under different filling conditions: (**a**) Sample No.1, (**b**) Sample No.2, (**c**) Sample No.3, (**d**) Sample No.4, and (**e**) Sample No.5

degree was less than for the initial stage. Since the filling material had been compacted in the early stage, the increase in confining stress had a relatively small effect on the flow channels in the fracture. As a result, the rate of decline in fracture transmissivity is less in the later confining stress stage.

Confining stress is another factor affecting fracture transmissivity, which has been well reported (Lee and Cho 2002; Liu et al. 2012b; Vogler et al. 2016). In the present study, a confining stress increment from 10 to 15 MPa resulted in a decrease in fracture transmissivity by about one order of magnitude, similar to what others have found. For example, Tan and Wang (2020) found in an experimental study that the permeability of the gypsum mortar-filled fracture was about 9×10^{-15} m^2 at a confining stress of 1.2 MPa, but at a confining stress of 10 MPa, it was reduced to 3×10^{-15} m^2, a reduction of about one order of magnitude. Nara et al. (2017) discovered that increasing confining stress from 2 to 10 MPa caused the permeability of unfilled fractures to decrease from 10^{-15} m^2 to 10^{-16} m^2, and the permeability of clay-filled fractures to decrease from 10^{-17} m^2 to 10^{-18} m^2. In this study, fracture transmissivity decreases more when confining stress is increased from 10 to 12 MPa, compared with when confining stress is increased from 12 to 15 MPa. This was also found by Jiang et al. (2020) who obtained a significantly greater reduction in permeability when the confining stress was increased from 3 to

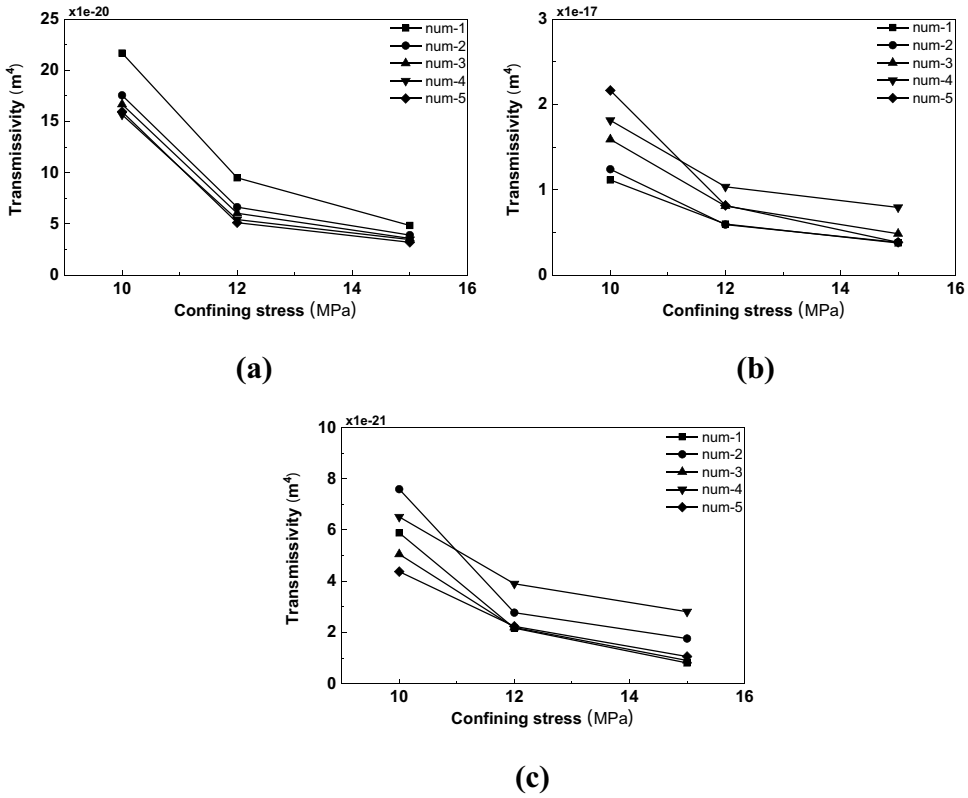

Fig. 10 Confining stress-transmissivity curves: (**a**) no filling; (**b**) filled with 100-mesh quartz sand; and (**c**) filled with bentonite

15 MPa (2.3×10^{-15} $m^2$to 1.05×10^{-15} m^2), larger decline than under a confining stress change from 15 to 35 MPa (1.05×10^{-15} m^2 to 0.6×10^{-15} m^2). All the results confirmed that the characteristics of the filling material can impact fracture transmissivity.

Effect of roughness

Unfilled fractures

Figure 11(a) shows that in the initial loading stage, the fracture transmissivity of unfilled fractures decreases with increasing roughness under the same level of confining stress. As the confining stress increased, this trend gradually diminished. The reason is that in the initial loading stage, rough fractures were the main flow channels. As shown in Fig. 4, greater roughness corresponds to more tortuous and longer flow paths. The energy consumed by the friction between the water and fracture surface would increase with increasing roughness which would reduce the flow capacity of fracture. At this point, the influence of roughness has a greater impact on fracture transmissivity, and greater roughness resulted in the lower transmissivity of unfilled fractures. In the later loading stage, high stress reduced the fracture aperture and the flow capacity, so the transmissivity effect of the flow path on the unfilled fracture decreased.

Fractures filled with sand

Figure 11(b) shows that for fractures filled with quartz sand, fracture transmissivity tended to increase with the increase of roughness during the initial loading stage. As the confining stress increased, this trend gradually diminished, indicating that the effect of roughness on the transmissivity of fracture filled with quartz sand was no longer dominant under high confining stress conditions. It is easier to cause the superposition of filling particles in the concave parts of the fracture surface with higher roughness, which would result in the increase of the fracture aperture due to the support of the filled sand. Therefore, in the initial loading stage, the pore structure was looser with high, the porosity with greater roughness. A high flow capacity of the fracture and larger transmissivity. With increasing confining stress, the pore structure of the filling medium would be compressed and thus reduce the flow capacity. This suggests that confining stress rather than the roughness plays a more significant role in fracture flow capacity.

Fractures filled with bentonite

Figure 11(c) shows that throughout the process of confining stress loading, the transmissivity of fractures filled with bentonite fluctuates with increasing roughness, with relatively

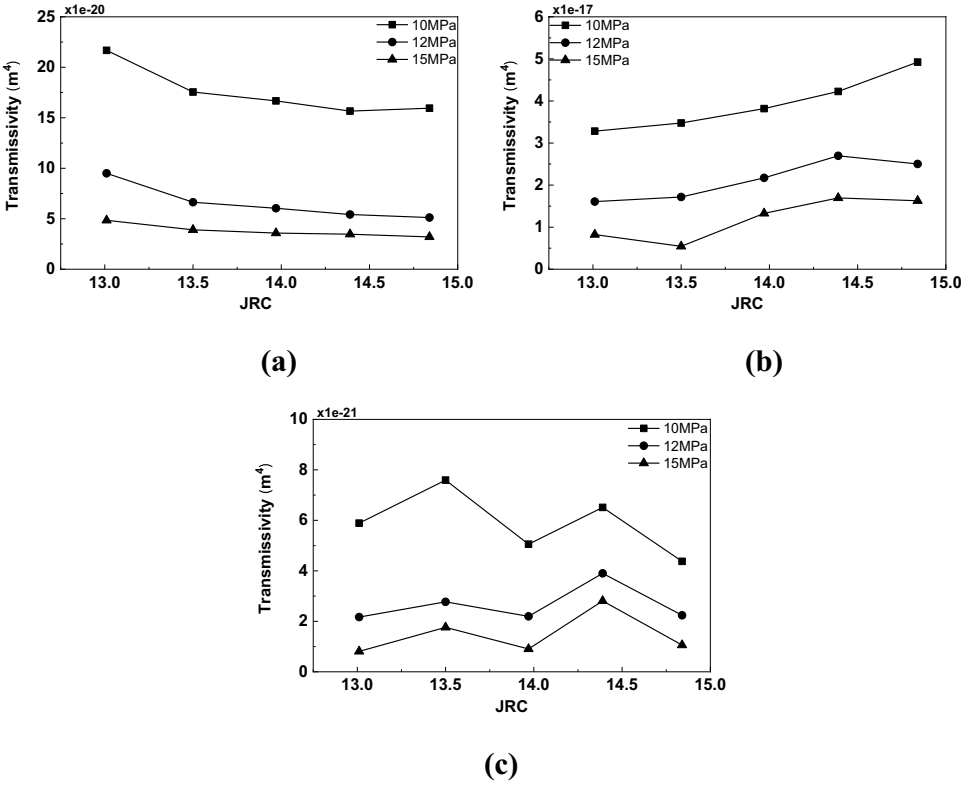

Fig. 11 JRC-transmissivity curves: (**a**) no filling, (**b**) filled with 50-mesh quartz sand, and (**c**) filled with bentonite

large variations. The reasons may be explained as follows. The water-blocking function of bentonite due to narrowing of the flow channel when bentonite was expanded after being exposed to water. Thus, flow rate and fracture transmissivity would be decreased. In the entire loading process, although the flow path of rough fracture is longer, because the fracture transmissivity is too low, the influence of the flow path length on fracture transmissivity was lost and the effect of roughness has a negligible effect on the transmissivity of fractures filled with bentonite.

According to the above analysis, the influence of fracture roughness on fracture transmissivity varies with filling conditions, as shown in Fig. 11, but the change in transmissivity is below one order of magnitude. A similar conclusion was given in other studies (Wang et al. 2019; Tan and Wang 2020), in which fracture width and filled of the fracture with dense gypsum mortar was studied. The permeability of filled fractures decreased with increasing roughness, but the change was less than one order of magnitude. To summarize, as the confining stress increased, the effect of roughness on fracture transmissivity gradually diminished.

This study assessed the effects of three factors on fracture transmissivity: filling condition, confining stress, and roughness. In future work, further consideration should be given to the effects of sample size and different mixtures of different filling materials on fracture transmissivity.

Conclusions

The results were presented of a series of tests on five artificially fractured granite samples to investigate the effects of filling condition, confining stress, and roughness on fracture transmissivity. The study could provide part of a basis for HLW repository safety assessment. The following conclusions may be drawn from this work.

The transmissivity of sand-filled fractures was the highest, while that of bentonite-filled fractures was the lowest. Compared with fractures without any filling material, fracture aperture is larger because of the filling sand, and coarser sand particles result in higher fracture transmissivity.

Higher confining stress reduces the transmissivity of the fracture, and the confining stress has a greater influence on the transmissivity of sand-filled fractures compared with other filling conditions. Conversely, for bentonite-filled fractures, the change in confining stress has little effect on the transmissivity.

The roughness of fracture surfaces is also one of the factors affecting the transmissivity of the samples, and the roughness has different effects on the fracture transmissivity for different filling conditions. Specifically, for unfilled fractures, higher roughness corresponds to lower fracture transmissivity, but for sand-filled fractures, the opposite is true, while the results for bentonite-filled samples are very scattered.

Funding This study was supported by the National Natural Science Foundation of China (Grant Nos. 51879260, 51879258, 11672099, and U1806226), CAS Interdisciplinary Innovation Team (JCTD-2018–17), the Key Research Program of the Chinese Academy of Sciences (Grant NO. KFZD-SW-423), and Hubei Provincial Natural Science Foundation of China (Grant No.2018CFA012).

Declarations

Competing interests The authors declare no competing interests.

References

Alam AKMB, Niioka M, Fujii Y, Fukuda D, Kodama J (2014) Effects of confining pressure on the permeability of three rock types under compression. Int J Rock Mech Min Sci 65:49–61. https://doi.org/10.1016/j.ijrmms.2013.11.006

Alireza B, Lanru J (2007) Hydraulic properties of fractured rock masses with correlated fracture length and aperture. Int J Rock Mech Min Sci 44:704–719. https://doi.org/10.1016/j.ijrmms.2006.11.001

Alireza B, Lanru J (2008) Stress effects on permeability in a fractured rock mass with correlated fracture length and aperture. Int J Rock Mech Min Sci 45:1320–1334. https://doi.org/10.1016/j.ijrmms.2008.01.015

Bandara KMAS, Ranjith PG, Rathnaweera TD (2020) Laboratory-scale study on proppant behaviour in unconventional oil and gas reservoir formations. J Nat Gas Sci Eng 78:103329. https://doi.org/10.1016/j.jngse.2020.103329

Blyth AR, Frape SK, Tullborg EL (2009) A review and comparison of fracture mineral investigations and their application to radioactive waste disposal. Appl Geochem 24:821–835

Chen Q, Kinzelbach W (2002) An NMR study of single- and two-phase flow in fault gouge filled fractures. J Hydrol 259:236–245. https://doi.org/10.1016/s0022-1694(01)00599-6

Cheng JY, Zhang HW, Wan ZJ (2018) Numerical simulation of shear behavior and permeability evolution of rock joints with variable roughness and infilling thickness. Geofluids 2018:1–11. https://doi.org/10.1155/2018/1869458

Coli N, Pranzini G, Alfi A, Boerio V (2008) Evaluation of rock-mass permeability tensor and prediction of tunnel inflows by means of geostructural surveys and finite element seepage analysis. Eng Geol 101:174–184. https://doi.org/10.1016/j.enggeo.2008.05.002

Hou TF, Zhang SC, Ma XF, Shao JJ, He YN, Lv XR, Han JY (2017) Experimental and theoretical study of fracture conductivity with heterogeneous proppant placement. J Nat Gas Sci Eng 37:449–461. https://doi.org/10.1016/j.jngse.2016.11.059

Indraratna B, Jayanathan M, Brown ET (2008) Shear strength model for overconsolidated clay-infilled idealised rock joints. Geotechnique 58:55–65. https://doi.org/10.1680/geot.2008.58.1.55

Indraratna B, Welideniya HS, Brown ET (2005) A shear strength model for idealised infilled joints under constant normal stiffness. Geotechnique 55:215–226. https://doi.org/10.1680/geot.55.3.215.61524

Jiang ZH, Wang HL, Xu JR, Chen HJ, Xie WC (2020) Variation of permeability of natural filled jointed rock under repeated loading and unloading conditions. Eur J Environ Civ Eng 2020:1–13. https://doi.org/10.1080/19648189.2020.1763846

Khosravi A, Serej AD, Mousavi SM, Haeri SM (2016) Effect of hydraulic hysteresis and degree of saturation of infill materials on the behavior of an infilled rock fracture. Int J Rock Mech Min Sci 88:105–114. https://doi.org/10.1016/j.ijrmms.2016.07.001

Lee HS, Cho TF (2002) Hydraulic characteristics of rough fractures in linear flow under normal and shear load. Rock Mech Rock Eng 35:299–318. https://doi.org/10.1007/s00603-002-0028-y

Li YW, Meng WN, Rui R, Wang JH, Jia D, Chen G, Patil S, Dandekar A (2018) The calculation of coal rock fracture conductivity with different arrangements of proppants. Geofluids 2018:1–10. https://doi.org/10.1155/2018/4938294

Liang TC, Cai B, Meng CY, Zhu XW, Liu YZ, Chen F (2021) The effect of proppant performance of hydraulic fracturing on conductivity. Fault-Block Oil & Gas Field 28(3):403–407

Liu J, Li JL, Wang RH, Zhu T, Qu JJ, Zhao ZY (2010) Experimental study of seepage in Yichang fractured sandstone with tight original rock fillings. Chin J Rock Mech Eng 29:366–374

Liu J, Li JL, Zhao ZY, Xiao L, Cai J (2012a) Research on seepage characteristics of splitting sandstone in different fillers and loading paths. Rock Soil Mech 33:45–47. https://doi.org/10.16285/j.rsm.2012.s2.002

Liu RC, Jing HW, He LX, Zhu TT, Yu LY, Su HJ (2017) An experimental study of the effect of fillings on hydraulic properties of single fractures. Environ Earth Sci 76(20):684. https://doi.org/10.1007/s12665-017-7024-8

Liu RC, Li B, Jiang YJ (2016) Critical hydraulic gradient for nonlinear flow through rock fracture networks: the roles of aperture, surface roughness, and number of intersections. Adv Water Resour 88:53–65. https://doi.org/10.1016/j.advwatres.2015.12.002

Liu RC, Li B, Jiang YJ, Yu LY (2018) A numerical approach for assessing effects of shear on equivalent permeability and nonlinear flow characteristics of 2-D fracture networks. Adv Water Resour 111:289–300. https://doi.org/10.1016/j.advwatres.2017.11.022

Liu XD, Luo TA, Zhu GP, Chen QC (2007) Study on properties of Gaomiaozi bentonite as the buffer/backfill material for HLW disposal. China Nuclear Science and Technology Report 02:140–156

Liu XY, Liu AH, Li XB (2012b) Experimental study of permeability of rock-like material with filling fractures under high confining pressure. Chin J Rock Mech Eng 31:1390–1398

Liu XY, Zhu ZD, Liu AH (2019) Permeability characteristic and failure behavior of filled cracked rock in the triaxial seepage experiment. Adv Water Resour 2019:1–12. https://doi.org/10.1155/2019/3591629

Lu YL, Wang LG, Li ZL, Sun HY (2016) Experimental study on the shear behavior of regular sandstone joints filled with cement grout. Rock Mech Rock Eng 50:1321–1336. https://doi.org/10.1007/s00603-016-1154-2

Liu YM, Chen ZR (2001) Bentonite from Gaomiaozi Inner Mongolia as an ideal buffer/backfilling material in handling highly radioactive wastes — a feasibility study. Acta Mineralogica Sinica 03:541–543

Majid NB, Lanru J (2015) Water pressure effects on strength and deformability of fractured rocks under low confining pressures. Rock Mech Rock Eng 48:971–985. https://doi.org/10.1007/s00603-014-0628-3

Min KB, Rutqvist J, Tsang CF, Jing LR (2004) Stress-dependent permeability of fractured rock masses: a numerical study. Int J Rock Mech Min Sci 41:1191–1210. https://doi.org/10.1016/j.ijrmms.2004.05.005

Mu WQ, Li LC, Yang TH, Yu GF, Han YC (2019) Numerical investigation on a grouting mechanism with slurry-rock coupling and shear displacement in a single rough fracture. Bull Eng Geol Env 78:6159–6177. https://doi.org/10.1007/s10064-019-01535-w

Nara Y, Kato M, Niri R, Kohno M, Sato T, Fukuda D, Daisuke F, Tsutomu S, Takahashi M (2017) Permeability of granite including macro-fracture naturally filled with fine-grained minerals. Pure Appl Geophys 175(3):917–927. https://doi.org/10.1007/s00024-017-1704-x

Olson JE, Laubach SE, Lander RH (2009) Natural fracture characterization in tight gas sandstones: Integrating mechanics and diagenesis. Bull Am Assoc Pet Geol 93:1535–1549. https://doi.org/10.1306/08110909100

Olsson R, Barton N (2001) An improved model for hydromechanical coupling during shearing of rock joints. Int J Rock Mech Min Sci 38:317–329. https://doi.org/10.1016/s1365-1609(00)00079-4

Pan ZQ, Qian QH (2009) Strategic research for deep geological disposal of high level radioactive waste. Atomic Energy Press, Beijing, China

Push R (2002) The Buffer and Backfill Handbook. Part 2: Materials and techniques. Geodevelopment AB. Technical Report TR-02–12. Svensk Kärnbränslehantering ABSE-102 40 Stockholm, Sweden

Rutqvist J (2015) Fractured rock stress-permeability relationships from in situ data and effects of temperature and chemical-mechanical couplings. Geofluids 15:48–66. https://doi.org/10.1111/gfl.12089

Shrivastava AK, Rao KS (2017) Physical modeling of shear behavior of Infilled rock joints under CNL and CNS boundary conditions. Rock Mech Rock Eng 51:101–118. https://doi.org/10.1007/s00603-017-1318-8

Suri Y, Islam SZ, Hossain M (2020) Effect of fracture roughness on the hydrodynamics of proppant transport in hydraulic fractures. J Nat Gas Sci Eng 103401. https://doi.org/10.1016/j.jngse.2020.103401

Tian X (2013) The study on geochemical characteristics of granite fracture fillings of geological disposal of high level radioactive waste in Beishan preselection area. Dissertation, Beijing Research Institute of Uranium Geology

Tan WH, Wang PF (2020) Experimental study on seepage properties of jointed rock-like samples based on 3D printing techniques. Advances in Civil Engineering 2020:1–10. https://doi.org/10.1155/2020/9403968

Vogler D, Amann F, Bayer P, Elsworth D (2016) Permeability evolution in natural fractures subject to cyclic loading and gouge formation. Rock Mech Rock Eng 49:3463–3479. https://doi.org/10.1007/s00603-016-1022-0

Wang GL, Liu WQ, Tao Y (2010) Experimental study of permeability in- fractured sandstone with sediment particles. Mechanics in Engineering 32:14–17

Wang J, Chen L, Su R, Zhao XG (2018) The Beishan underground research laboratory for geological disposal of high-level radioactive waste in China: planning, site selection, site characterization and in situ tests. J Rock Mech Geotech Eng 10:411–435. https://doi.org/10.1016/j.jrmge.2018.03.002

Wang J, Chen WM, Su R, Guo YH, Jin YX (2006) Geological disposal of high-level radioactive waste and its key scientific issues. Chin J Rock Mech Eng 25:801–812

Wang L, Liu JF, Pei JL, Xu HN, Bian Y (2015) Mechanical and permeability characteristics of rock under hydro-mechanical coupling conditions. Environ Earth Sci 73:5987–5996. https://doi.org/10.1007/s12665-015-4190-4

Wang M, Chen YF, Ma GW, Zhou JQ, Zhou CB (2016) Influence of surface roughness on nonlinear flow behaviors in 3D self-affine rough fractures: Lattice Boltzmann simulations. Adv Water Resour 96:373–388. https://doi.org/10.1016/j.advwatres.2016.08.006

Wang PF, Tan WH, Ma XW, Li ZJ, Liu JJ, Wu YF (2019) Experimental study of seepage characteristics of consecutive and filling fracture with different roughness levels and gap-widths. Rock Soil Mech 40:3062–3070

Wealthall GP, Steele A, Bloomfield JP, Moss RH, Lerner DN (2001) Sediment filled fractures in the Permo-Triassic sandstones of the Cheshire Basin: observations and implications for pollutant transport. J Contam Hydrol 50:41–51. https://doi.org/10.1016/s0169-7722(01)00104-8

Wu J, Yin Q, Jing H (2020) Surface roughness and boundary load effect on nonlinear flow behavior of fluid in real rock fractures. Bull Eng Geol Env 79:4917–4932. https://doi.org/10.1007/s10064-020-01860-5

Xiao H, Li ZM, He SY, Lu XQ, Liu PL, Li J (2021) Experimental study on proppant diversion transportation and multi-size proppant distribution in complex fracture networks. J Pet Sci Eng 196:107800. https://doi.org/10.1016/j.petrol.2020.107800

Xu JX, Ding YH, Yang LF, Liu Z, Gao R, Yang HX, Wang Z (2019) Conductivity analysis of hydraulic fractures filled with non-spherical proppants in tight oil reservoir. Energy Sci Eng 8:166–180. https://doi.org/10.1002/ese3.517

Yang DS, Wang W, Li K, Chen WZ, Yang JP, Wang SG (2019) Experimental investigation on the stress sensitivity of permeability in naturally fractured shale. Environ Earth Sci 78(2):55. https://doi.org/10.1007/s12665-019-8045-2

Yang SQ, Ranjith PG, Jing HW, Tian WL, Ju Y (2017) An experimental investigation on thermal damage and failure mechanical behavior of granite after exposure to different high temperature treatments. Geothermics 65:180–197. https://doi.org/10.1016/j.geothermics.2016.09.008

Yang SQ, Tian WL, Huang YH (2018) Failure mechanical behavior of pre-holed granite specimens after elevated temperature treatment by particle flow code. Geothermics 72:124–137. https://doi.org/10.1016/j.geothermics.2017.10.018

Yang ZY, Lo SC, Di CC (2001) Reassessing the joint roughness cofficient (JRC) estimation using Z_2. Rock Mech Rock Eng 34:243–251. https://doi.org/10.1007/s006030170012

Ye F, Duan JC, Fu WX, Yuan XY (2019) Permeability properties of jointed rock with periodic partially filled fractures. Geofluids 2019:1–14. https://doi.org/10.1155/2019/4039024

Yin Q, Jing HW, Ma GW, Su HJ, Liu RC (2019) Laboratory investigation of hydraulic properties of deformable rock samples subjected to different loading paths. Hydrogeol J 27:2617–2635. https://doi.org/10.1007/s10040-019-02015-x

Yu J, Chen X, Cai YY, Li H (2015) Triaxial test research on mechanical properties and permeability of sandstone with a single joint filled with gypsum. Korean Society of Civil Engineers Journal of Civil Engineering 20:2243–2252. https://doi.org/10.1007/s12205-015-1663-7

Yong R, Ye J, Li B, Du SG (2018) Determining the maximum sampling interval in rock joint roughness measurements using Fourier series. Int J Rock Mech Min Sci 101:78–88. https://doi.org/10.1016/j.ijrmms.2017.11.008

Zhang S, Ye F, Fu WX, Zheng S (2021) Critical hydraulic gradient of piping erosion under free and seepage flow coupling model. International Journal of Geomechanics 21(6):04021069. https://doi.org/10.1061/(ASCE)GM.1943-5622.0002026.

Zhao XG, Wang J, Ma LK, Su R, Jin YX, Chen QC, An QM, Qin XH (2014) Distribution characteristics of geostress field in Xinchang rock block of candidate Beishan area for high level radioactive waste repository in China. Chin J Rock Mech Eng 33(S2):3750–3759

Zheng WB, Silva SC, Tannant DD (2018) Crushing characteristics of four different proppants and implications for fracture conductivity. J Nat Gas Sci Eng S1875510018300982. https://doi.org/10.1016/j.jngse.2018.02.028

Zheng XJ, Chen M, Hou B, Ye ZH, Wang W, Yin CB, Chen XY (2016) Effect of proppant distribution pattern on fracture conductivity and permeability in channel fracturing. J Petrol Sci Eng S0920410516306933. https://doi.org/10.1016/j.petrol.2016.10.023

Zheng XQ, Wang X, Zhang FX, Yang NY, Cai B, Liang TC, Meng CY, Lu HB, Yi XB, Yan YZ, Wang JT, Jiang W, Wang TY (2021) Domestic sand proppant evaluation and research progress of sand source localization and its prospects. China Petroleum Exploration 26(01):131–137

Zhu WY, Liu Q, Ming Y, Zhang LY (2019) Calculation of fracture conductivity considering proppant influence and simulation of proppant transport in fracture. Chemical Engineering of Oil & Gas 48(02):75–78

Zimmerman RW, Bodvarsson GS (1996) Hydraulic conductivity of rock fractures. Journal of Transport in Porous Media 23(1):1–30